Inhomogeneous big-bang nucleosynthesis in light of recent observations

Kimmo Kainulainen*
NORDITA, Blegdamsvej 17, DK-2100, Copenhagen Ø, Denmark

Hannu Kurki-Suonio†
Helsinki Institute of Physics, P.O. Box 9, FIN-00014 University of Helsinki, Finland

Elina Sihvola‡
Department of Physics, P.O. Box 9, FIN-00014 University of Helsinki, Finland
(Received 14 July 1998; published 18 March 1999)

We consider inhomogeneous big-bang nucleosynthesis in light of the present observational situation. We give updated limits to the baryon-to-photon ratio and Ω_b and show that the inhomogeneous nucleosynthesis may alleviate the tension between ^{4}He and D observations. The recent Kamiokande results are shown to strongly disfavor the decaying τ neutrino solution to this tension. The possible sources of baryon inhomogeneity include the QCD and electroweak phase transitions (EWPT). It is found that EWPT produces a distinct ''beer foam'' geometry of inhomogeneity, but that the distance scale is too small for them to have a large effect on nucleosynthesis; the effect may still be larger than some of the other small corrections recently incorporated to SBBN codes. [S0556-2821(99)01108-X]

PACS number(s): 98.80.Ft, 26.35.+c, 98.80.Cq

I. INTRODUCTION

Standard big-bang nucleosynthesis [1–3] (SBBN) predicts the primordial abundances of D, ^{3}He, ^{4}He, and ^{7}Li as a function of a single parameter, the baryon-to-photon ratio $\eta \equiv n_b/n_\gamma$, which is related to the baryonic mass-density parameter $\Omega_b \equiv 8\pi G\rho_{b0}/3H_0^2$ by

$$\Omega_b h^2 = 3.70\times 10^{-3}\eta_{10}, \tag{1}$$

where $\eta_{10} \equiv 10^{10}\eta$ and $h \equiv H_0/100$ km s^{-1}Mpc^{-1}. The observed abundances of these isotopes are in rough agreement with the SBBN predictions [4] for a range of η_{10}, which is compatible with other cosmological bounds on the amount of baryonic matter in the universe. In principle, comparing SBBN predictions with primordial abundances extrapolated from observations pins down the precise value of η_{10}. A few years ago the standard result was $\eta_{10}\sim 3-4$ [2,3], but even much tighter constraints were published (e.g., $2.69 \leqslant \eta_{10} \leqslant 3.12$ [5]). Recently the situation has become more complicated, and it seems that such precise determinations may have been premature.

Since the discovery of the τ lepton, implying three flavors of light neutrinos, there has been tension between ^{4}He and D in SBBN [6,7]. Olive *et al.* [8] (OSS97) have reviewed the ^{4}He observations and their best estimate is

$$Y_p = 0.230 \pm 0.003. \tag{2}$$

This corresponds to $\eta_{10} = 1.4 \pm 0.3$ and hence to primordial D/H$\sim 2-3\times 10^{-4}$ in SBBN, whereas the present D/H in the interstellar medium (ISM) is [9] only 1.5×10^{-5}. Most models of galactic chemical evolution have difficulty explaining this much deuterium astration [10], and prefer a much lower primordial D/H and thus a higher baryon density, $\eta_{10}\sim 5$.

The conventional way to deal with this tension has been to compromise by settling on an intermediate η_{10} which is preferred neither by ^{4}He nor by D/H but is considered acceptable to both. This, however, leads to an artificially high precision in the η_{10} determination, because while the individual ranges in η_{10} accepted by ^{4}He and D/H are wide, their overlap is narrow. Tension increased when data were subjected to more thorough formal statistical analysis, culminating in a claim of a ''crisis'' in SBBN, by Hata *et al.* [11], who concluded that given the existing data the overlap is in fact nonexistent.

In the context of SBBN the resolution of this crisis requires either a revision of the picture of the galactic chemical evolution [12], so that much more deuterium astration can be accommodated [13], or a large systematic error in the Y_p determination [4,14]. Indeed, based on a number of new ^{4}He observations, Izotov and Thuan [15] have claimed a significantly higher Y_p than the 1997 result of Olive, Steigman, and Skillman [8] (OSS97):

$$Y_p = 0.244 \pm 0.002. \tag{3}$$

Whether this new value is to be accepted as such is yet unclear, since several sources of poorly known systematic effects are expected to contribute to the discrepancy [16].

Interestingly, some particle physics solutions based on a massive decaying tau neutrino [17] can now be ruled out using the recent results from Kamiokande [18]. The directional dependence in the upward-going muon neutrino deficiency seen in the Super Kamiokande experiment is a strong implication that the muon neutrinos undergo oscillations

*Email address: Kimmo.Kainulainen@nbi.dk
†Email address: Hannu.Kurki-Suonio@helsinki.fi
‡Email address: Elina.Sihvola@helsinki.fi

while traversing through the Earth. This implies that ν_μ mixes with either a tau neutrino or a new sterile neutrino with a mass splitting of about $\delta m^2 \sim 10^{-3}$ eV^2 and with an almost maximal mixing angle. If this mixing is between ν_μ and ν_τ, then ν_τ is obviously light so that the scenarios based on heavy ν_τ decaying into ν_μ and some scalar particle [17] are immediately ruled out. Suppose then that the atmospheric anomaly is due to mixing between ν_μ and some sterile neutrino. Now ν_τ can be heavy and having it decay away to a muon neutrino and a scalar state prior to nucleosynthesis could alleviate the tension somewhat. The effect is roughly equivalent to having about a half a neutrino degree of freedom worth less energy density in the universe [17] (less energy density leads to slower expansion and, hence, later decoupling of the n/p ratio). However, the sterile state with the requested mixing parameters is brought into full thermal equlibrium due to oscillation and quantum damping prior to nucleosynthesis [19], overcoming the alleviating effect discussed above and making the tension even worse. The only possibility to alleviate the tension is that $m_{\nu_\tau} \sim$ few MeV and ν_τ decays into an *electron neutrino* in the short interval after the electron neutrino freeze-out but prior to the onset of nucleosynthesis. In this case the excess (almost thermal) electron neutrinos can significantly increase the weak interaction rates keeping the n/p ratio in equilibrium longer and hence leading to much less helium being produced [20,21]. Bringing the sterile neutrino into equilibrium makes also this solution less effective, but is not strong enough to rule out the possibility entirely [21,22].

The chemical evolution of D and ^{4}He is particularly simple: ^{4}He increases with time, whereas D decreases. In contradistinction, ^{3}He and ^{7}Li are both produced and destroyed during galactic chemical evolution. This makes it difficult to estimate their primordial abundances.

For ^{7}Li there is a very impressive plateau [23] of abundances in PopII stars. The observed value is [24,25] $\log_{10}(^7\mathrm{Li/H}) = -9.75 \pm 0.10$. The universality of this abundance suggests that it is closely related to the primordial abundance. There may have been some depletion; i.e., some of the surface ^{7}Li has been destroyed by the star. Pinsonneault *et al.* [25] estimate a depletion factor $D_7 = 0.2$–0.4 dex. This corresponds to a primordial

$$\log_{10}(^7\mathrm{Li/H})_p = -9.45 \pm 0.20. \tag{4}$$

However, Vauclair and Charbonnel [26] give a lower estimate

$$\log_{10}(^7\mathrm{Li/H})_p = -9.65 \pm 0.10. \tag{5}$$

These estimates for lithium are compatible with either a low, $\eta_{10} \sim 1.5$, or a high, $\eta_{10} \sim 4-6$ baryon density, but disfavor a compromise value $\eta_{10} \sim 2.5-3$.

A promising new method with the potential to resolve this η dicothomy is the observation of (the presumably primordial abundance of) deuterium in clouds at high redshifts by their absorption of quasar light. Unfortunately, at present we only have a small number of such D/H measurements, and even the existing ones are still controversial. Burles and Tytler [27] obtain from their two best observations

$$\mathrm{D/H} = 3.4 \pm 0.3 \times 10^{-5}, \tag{6}$$

which corresponds to $\eta_{10} = 5.1 \pm 0.3$ in SBBN. However, the analysis of Burles and Tytler has been debated [28] and one observation by HST [29] from an absorption cloud at $z = 0.7$ appears to give a *high* value of $\mathrm{D/H} \sim 2 \times 10^{-4}$.

Thus the observational situation remains unclear. If we suppose that some of the determinations of primordial abundances are correct, but we do not know which, we are led to a SBBN range

$$\eta_{10} \sim 1.5-6. \tag{7}$$

In conclusion, there is an unsettled disagreement between different observations in the context of SBBN. While the problem may lie with the observations or in the determination of primordial abundances from them, another possibility is that the primordial abundances indeed do not correspond to the same η in SBBN, so that it needs to be modified. In this paper we study the possibility of inhomogenous big-bang nucleosynthesis (IBBN) in light of the present observational situation. In Sec. II we discuss the generic mechanisms known to produce inhomogeneities in the baryon distribution and the significance of the distance scale of the inhomogeneity. We describe our numerical calculations in Sec. III and give our results in Sec. IV. Section V contains our conclusions.

II. GENERATING THE INHOMOGENEITY

Various phase transitions which took place before nucleosynthesis were capable of producing large-amplitude small-scale fluctuations in the baryon number density: in particular the electroweak (EW) transition at $T \sim 100$ GeV and $t \sim 10^{-11}$ s and the QCD transition at $T \sim 150$ MeV and $t \sim 10^{-5}$ s.

IBBN was studied extensively in the late 1980s, when it was realized that a first-order QCD transition could produce the kind of inhomogeneity which would affect BBN [30–32]. The original mechanism relying on chemical pressure [34], operative in the QCD transition, leads to a geometry where localized clumps of high density are surrounded by large voids of low baryon density [35,36]. The details of the QCD transition are poorly known and both the amplitude and the size of the inhomogeneities can vary significantly; the size of course is bounded by the horizon at the QCD transition, which is about 2×10^6 m (at $T = 1$MeV) $= 0.4$ pc (today).

Also the electroweak phase transition (EWPT) generically produces inhomogeneities and possibly with large density contrasts. This assumes of course that the baryons we see around us today were generated during the electroweak phase transition [37]. Some scenarios [38,39] may even give rise to regions of antibaryons mixed with the overall baryonic excess, leading to the interesting possibility of nucleosynthesis in the presence of antibaryons [40,41]. The generic feature leading to the formation of inhomogeneities in the

more standard scenarios is the strong dependence of the baryoproduction rate on the bubble wall velocity in the so-called ''charge transport mechanism'' [42], coupled with the characteristic changes in the velocity of the bubble walls during the transition [43]. For thin walls one finds a local baryoproduction rate

$$B(x) \approx c/v_w(x). \tag{8}$$

The velocity dependence of the local baryoproduction rate due to the ''classical chiral force'' mechanism [44], operative in the limit of wide walls, is much weaker [45]. However, the generic geometry of inhomogeneities arising from the EWPT is quite the opposite to the QCD case: voids of low density surrounded by walls of high density.

After nucleation bubble walls quickly accelerate to a terminal velocity $v_w \sim (0.1-0.5)c$, whose exact value depends on the parameters of the phase transition, such as the latent heat released, the surface tension, and the frictional forces effected on the bubble wall by the ambient plasma [46,47]. After some time (we are only considering deflagration bubbles here), the shock waves preceding phase transition fronts collide reheating the unbroken phase plasma back to the critical temperature. As a result the pressure forces driving the bubble expansion are reduced and, were it not for the general expansion of the universe, the walls would come to a complete stop. Because of Hubble expansion, the walls can still continue expanding, but now with a greatly reduced speed, typically $v_w \sim \mathcal{O}(\text{few}) \times 10^{-3} c$ [47]. These velocity scales and the rate (8) indicate that the maximal density contrast possibly generated by the EW mechanism is about ~ 100.

The typical size of the voids in this ''beer foam'' geometry is some fraction of the horizon at the EW transition, $l_H = 3 \times 10^3$ m (at 1 MeV) $= 6 \times 10^{-4}$ pc (today). A nucleation calculation, which ignores the thermodynamics of the bubble interactions, typically gives for the size of bubbles at the coalescence only $l_b \sim 10^{-3} l_H$ [47–49]. However, as a result of reheating, the first nucleated bubbles may inhibit the growth of bubbles formed only slightly later, increasing perhaps significantly the size of the largest structures as compared with the simplest nucleation estimate. Also in extended scenarios including magnetic fields [39], the size of a single bubble can reach the horizon scale. We then consider the inhomogeneity size a free parameter, with values $r \sim 10^{-3} - 1 l_H$.

Both the EW and QCD transitions appear capable of producing high initial density contrasts. In both cases the density fluctuations would be non-Gaussian, consisting of high- and low-density regions. The pattern would not be regular, but it would have a characteristic distance scale. The inhomogeneity can be described by the typical geometric shape of these regions and the following three parameters: (1) typical distance scale r, (2) typical density contrast $R \equiv \eta_{\text{high}}/\eta_{\text{low}}$, and (3) the volume fraction f_v of the high-density regions.

The distance scale r is especially important. An inhomogeneity can have a large effect on nucleosynthesis only if the distance scale is comparable to the neutron diffusion length d_n during nucleosynthesis. QCD-scale inhomogeneities could be [36] of the scale required, although QCD lattice calculations [50] favor values below the short end of this range. For the EW case this range corresponds to a fluctuation scale $r \gtrsim 0.1 l_H$ during the transition.

There may be other possible sources of baryon inhomogeneity in addition to the EW and QCD phase transitions. Moreover, there is a considerable uncertainty regarding the parameters r, R, and f_v from each transition. Therefore it is natural to treat the two questions separately: (1) Are there IBBN parameter regions where IBBN agrees with observations equally well or better than SBBN? (2) Could the EW or QCD phase transition produce inhomogeneity in this parameter region?

III. COMPUTATIONS

The IBBN code used for this paper is based on the code used in [31] and the nuclear reaction rates have been updated according to [3]. In the ^{4}He yield we take into account the various corrections to the weak reaction rates [7,5,51]. We also take into account the theoretical uncertainty in the ^{7}Li yields [3].

We assume spherical symmetry and use a nonuniform radial grid of 64 zones representing a sphere with comoving radius r, with reflective boundary conditions both at the center and at r. This setup allows us to model both geometries discussed above: the centrally condensed density describes the QCD-type geometry and spherical shells of high density describe the EW-type geometry. The volume fraction covered by the high-density region in each geometry is

$$f_v = f_r^3 \quad \text{(centrally condensed)}, \tag{9}$$

$$f_v = 1 - (1 - f_r)^3 \quad \text{(spherical shell)}, \tag{10}$$

where f_r denotes the fraction of the radius covered by the high-density region. Given the geometry, the model is specified by four parameters: r, f_v, R described above, and the average baryon-to-photon ratio η.

The most dramatic effect is obtained when the neutron diffusion out of the high-density region leads to a large excess of neutrons in the low-density region. This requires a density contrast

$$R \gg \left(\frac{p}{n}\right)_0 \frac{1}{f_v}, \tag{11}$$

where $(p/n)_0 \sim 7$ is the SBBN proton/neutron ratio at the onset of nucleosynthesis. Increasing R further leads to a stronger effect, but the increase soon saturates, and one gets almost a maximal effect at $R = 20/f_v$ already. In most cases we chose to run with large enough R to have close to this maximal effect. This leaves us with three parameters f_v, η, r. We did runs with 11 different values of f_v altogether (Table I).

For the runs with spherical shell geometry, we kept $R = 1000$ constant. For the centrally condensed geometry some

TABLE I. The different geometries studied. R is the density contrast between the high and low density, f_r is the high-density fraction of the grid radius, and f_v is the corresponding volume fraction.

R	f_r	f_v	$f_v R$
	Centrally condensed (c.c.)		
283	$1/\sqrt{2}$	0.3536	100
800	1/2	0.125	100
2263	$1/2\sqrt{2}$	0.0442	100
6400	1/4	0.0156	100
51200	1/8	0.0020	100
	Spherical shell (s.s.)		
1000	1/4	0.5781	578
1000	1/8	0.3301	330
1000	1/16	0.1760	176
1000	1/32	0.0909	91
1000	1/64	0.0461	46
1000	1/128	0.0233	23

of the volume fractions were so small that a larger R was needed to get the large inhomogeneity effect. For the centrally condensed runs we kept the product $f_v R = 100$ constant instead.

IV. RESULTS

It has been customary in IBBN studies [32,33] to plot the regions in the (η, r) plane allowed by different observational constraints. Since the observational situation has become rather less clear recently, we present the results first as abundance contours for a given f_v, so the different constraints can then be applied afterwards. For ^{4}He we plot the mass fraction Y_p; for D and ^{7}Li we plot the number ratios D/H and ^{7}Li/H. To save space, the less interesting ^{3}He is not shown. In Figs. 1 and 2 we present the results for the centrally condensed (c.c.) runs with $f_r = 1/2$ and $f_r = 1/4$. The results from other runs described in Table I are qualitatively similar. In the spherical shell (s.s.) geometry the distance scales where one gets the strongest effects are larger than in the c.c. geometry.

It is clear that at the distance scales attainable in the EW transition (indicated by the lower horizontal dashed line in the figures) the IBBN results do not significantly differ from SBBN results; the observational uncertainties are certainly much larger. However, even with scales as small as $r \sim 0.05 l_H$, the effect of inhomogeneity (see Fig. 3) can be larger than certain small corrections recently included into the SBBN computations [51].

A. Optimum scales

How much ^{4}He is produced depends on the number of neutrons available. The yield is minimized at an optimum distance scale $r_{\rm opt} \sim 10^4$–10^5 m, where a maximal number of neutrons diffuse out from the high-density region (where most of the ^{4}He is produced), but not too many of them

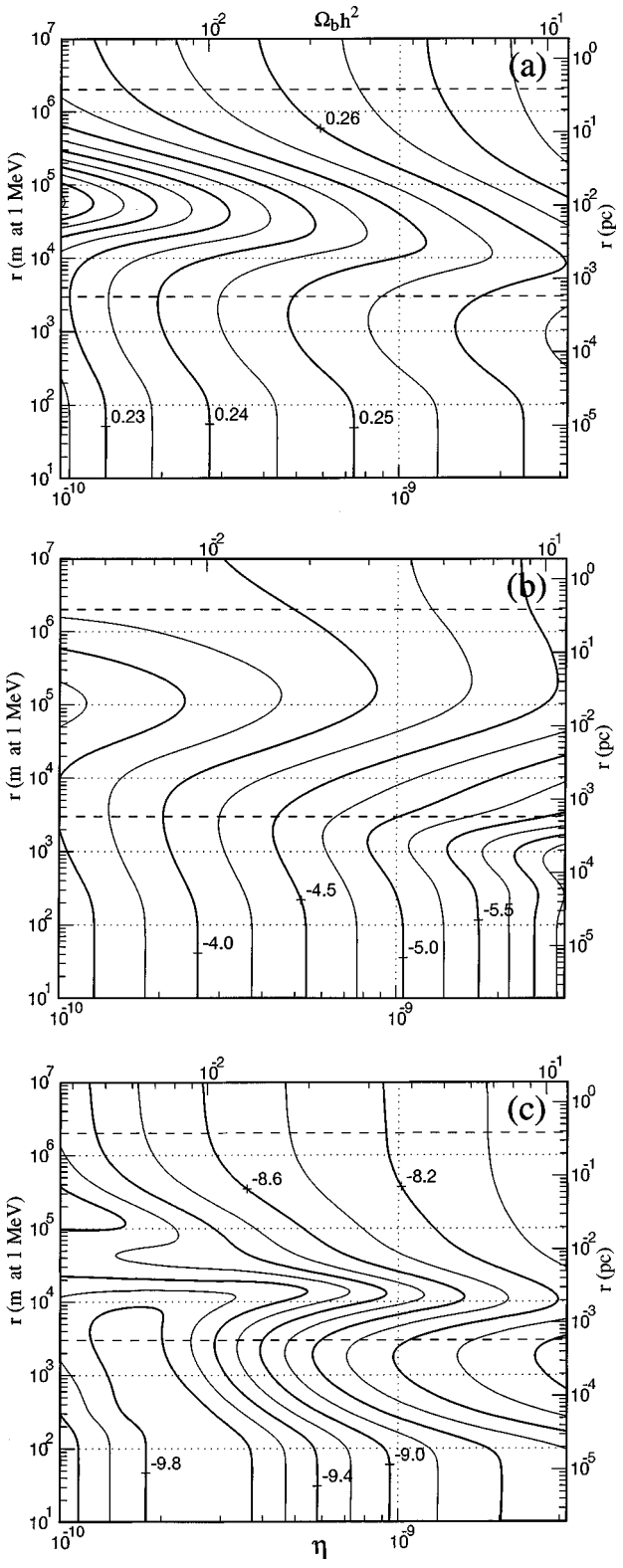

FIG. 1. The ^{4}He, D, and ^{7}Li yields from inhomogeneous nucleosynthesis runs with the centrally condensed geometry, with $R = 800$ and $f_r = 1/2$ ($f_v = 0.125$). The contours of (a) Y_p, (b) $\log_{10}$D/H, and (c) $\log_{10}{}^7$Li/H are plotted as a function of the average baryon-to-photon ratio η and the distance scale r of the inhomogeneity. The two horizontal dashed lines denote the horizon scale l_H at the QCD (upper) and EW (lower) phase transitions.

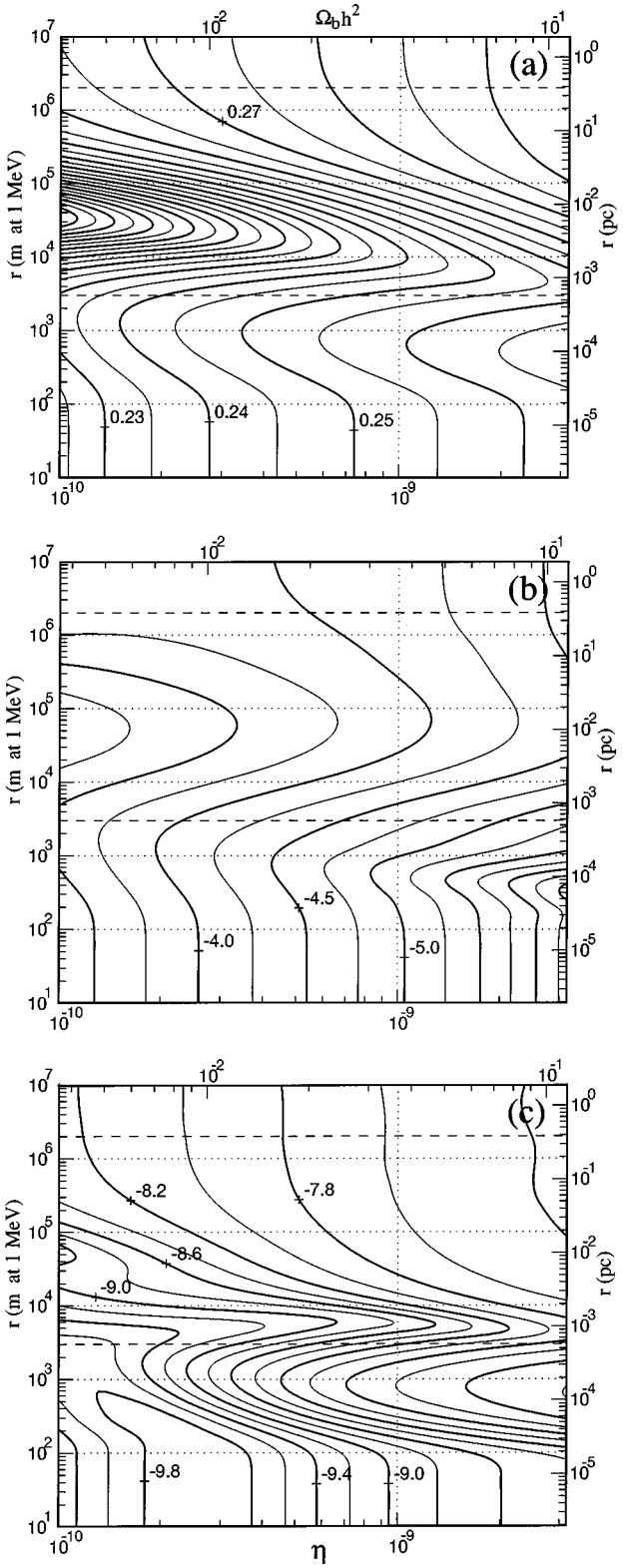

FIG. 2. Same as Fig. 1, but for $R=6400$ and $f_r=1/4$ ($f_v=0.0156$).

diffuse back when the nucleosynthesis in the high-density region starts consuming free neutrons.

We find that $r_{\rm opt}$ goes down with increasing η, roughly as $\eta^{-2/3}$. Also, the s.s. geometry gives a larger optimum scale

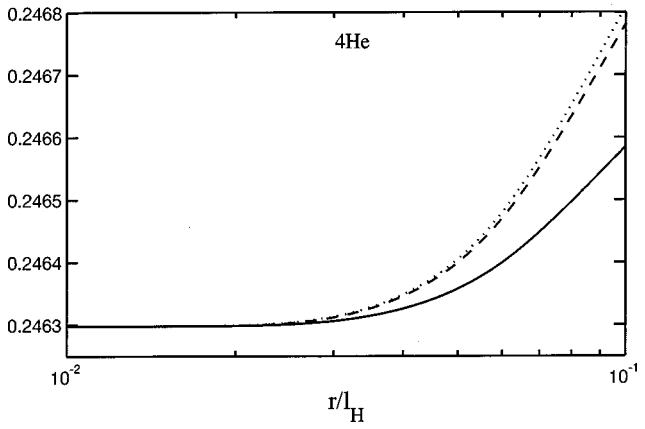

FIG. 3. Effects of small-scale inhomogeneity on the ^{4}He yield. This figure is for the spherical shell geometry appropriate for the EW transition, and for $f_v=0.3301$ and $\eta_{10}=5$. The three lines correspond to $R=10$ (solid line), 100 (dashed line), and 1000 (dotted line) (or $f_vR=3.3,33,330$), showing how the effect saturates for large R, so that there is little difference between $R=100$ and $R=1000$. The horizontal axis gives the ratio of the distance scale to the EWPT horizon.

than does the c.c. geometry with the same f_v, and the dependence on f_v is different with different geometries: for centrally condensed spheres $r_{\rm opt}$ goes down with decreasing f_v, whereas for spherical shells it increases with decreasing f_v.

It is possible to derive the parametric dependence of $r_{\rm opt}$ on η and f_v analytically. Consider the diffusion of neutrons after the weak freeze-out but before the start of nucleosynthesis. The flux of neutrons into the low-density region is proportional to the neutron diffusion coefficient D, to the surface area A of the boundary, and to the gradient of the neutron density at the boundary, roughly $(n_{\rm high}-n_{\rm low})/\sqrt{Dt}$. Here $\sqrt{Dt}$ is the diffusion length of neutrons, and $n_{\rm high}$ and $n_{\rm low}$ are the average neutron densities in the high- and low-density regions, respectively. $n_{\rm high}$ decreases as

$$V\frac{\partial n_{\rm high}}{\partial t}\sim -AD\frac{n_{\rm high}-n_{\rm low}}{\sqrt{Dt}}, \tag{12}$$

where V is the volume of the high-density region. If we ignore nuclear reactions and weak inteactions, we can integrate out Eq. (12):

$$n_{\rm high}-n_{\rm low}\sim\exp\left(-\frac{A}{V}\frac{\sqrt{Dt}}{(1-f_v)}\right). \tag{13}$$

The optimum scale corresponds to

$$\frac{A}{V}\frac{\sqrt{Dt_{\rm ns}}}{(1-f_v)}\sim 1, \tag{14}$$

where $t_{\rm ns}$ is the starting time of nucleosynthesis. At scales larger than the optimum scale, the neutrons have not diffused out effectively before the synthesis of ^{4}He begins. On the

other hand, making the scale smaller than the optimum scale does not significantly increase the number of neutrons diffusing out, but makes the back-diffusion at later times more effective.

Now it is easy to see why the optimum scales are smaller for condensed spheres. For the same f_v, the surface-to-volume ratio A/V is smaller for condensed spheres than for shell geometry, which makes the out-diffusion less effective and optimum scales smaller.

The η dependence of the optimum scale is through the dependence on the diffusion length. The diffusion at the boundary is controlled by the smaller diffusion coefficient of the high-density region. The diffusion is dominated by scattering on protons, $D_{np} < D_{ne}$. After electron-positron annihilation the diffusion constant depends on the proton density and temperature as

$$D_n \simeq D_{np} \propto \frac{1}{\eta_{\rm high} T^{5/2}} \approx \frac{f_v}{\eta T^{5/2}}. \tag{15}$$

The starting temperature $T_{\rm ns}$ of nucleosynthesis depends on $\eta_{\rm high}$. The dependence in the range $\eta_{\rm high} = 10^{-10}$–$10^{-8}$ is $T_{\rm ns} \propto \eta_{\rm high}^{\gamma}$, $\gamma = 0.07$–0.1. Thus the diffusion length should go as

$$\sqrt{D t_{\rm ns}} \propto \eta_{\rm high}^{-1/2} T_{\rm ns}^{-9/4} \propto n_{\rm high}^{-1/2-9\gamma/4} = n_{\rm high}^{-\alpha}, \tag{16}$$

where $\alpha = 0.65 - 0.73 \sim 2/3$, so that for the optimum scale

$$(1-f_v)\frac{V}{A} \propto \eta_{\rm high}^{-2/3}. \tag{17}$$

The surface-to-volume ratio of the high-density region is

$$\frac{A}{V} = \frac{3}{f_v^{1/3} r} \quad \text{(c.c.)}, \tag{18a}$$

$$\frac{A}{V} = \frac{3}{r}\frac{(1-f_v)^{2/3}}{f_v} \quad \text{(s.s.)}. \tag{18b}$$

Combining Eqs. (17) and (18) we find the observed behavior for the optimum scale:

$$r_{\rm opt} \propto \frac{f_v^{1/3}}{(1-f_v)}\,\eta^{-2/3} \quad \text{(c.c.)}, \tag{19a}$$

$$r_{\rm opt} \propto \frac{\eta^{-2/3}}{f_v^{1/3}(1-f_v)^{1/3}} \quad \text{(s.s.)}. \tag{19b}$$

B. Constraints on η

We now compare our IBBN yields to observational constraints. Since at present there is no agreement about what constraints to use, we consider a number of different sets of constraints.

The most fundamental abundance constraints are the upper limit to primordial ^{4}He and the lower limit to primordial D/H, obtained directly from observed abundances, since chemical evolution always increases the ^{4}He abundance and reduces D/H. So in our first set we conservatively take for ^{4}He the 2σ upper limit by Izotov and Thuan [15],

$$Y_p \leqslant 0.248, \tag{20}$$

and for D/H we use the present ISM abundance [9] as the lower limit:

$$\mathrm{D/H} \geqslant 1.5 \times 10^{-5}. \tag{21}$$

It turns out that all our IBBN models which satisfy Eq. (20) satisfy Eq. (21) also. In Fig. 4 we have plotted the contour (20) from the c.c. models. In SBBN the constraint (20) gives an upper limit to η, $\eta_{10} \leqslant 6.3$. We see that IBBN raises this upper limit to

$$\eta_{10} \leqslant 19, \quad \text{or} \quad \Omega_b h^2 \leqslant 0.07. \tag{22}$$

Similar results were obtained for the s.s. geometry.

While IBBN raises the upper limit to η from ^{4}He and D/H by a factor of 2–3, upper limits from ^{7}Li are raised at most by a factor of 1.4 and, if we choose a very tight ^{7}Li limit, not at all. Thomas *et al.* [33] used $^7\mathrm{Li/H} < 1.4 \times 10^{-10}$, which gives them a SBBN upper limit $\eta_{10} \leqslant 3.1$, and this limit was not relaxed at all by IBBN. We confirm that none of our IBBN models raises the upper limit to η from this constraint. However, their upper limit for ^{7}Li allows essentially no depletion at all.

As our second set we take the case for a high η based on the high-z deuterium value of Burles and Tytler [27]. We use the 2σ range

$$\mathrm{D/H} = 3.4 \pm 0.6 \times 10^{-5} \tag{23}$$

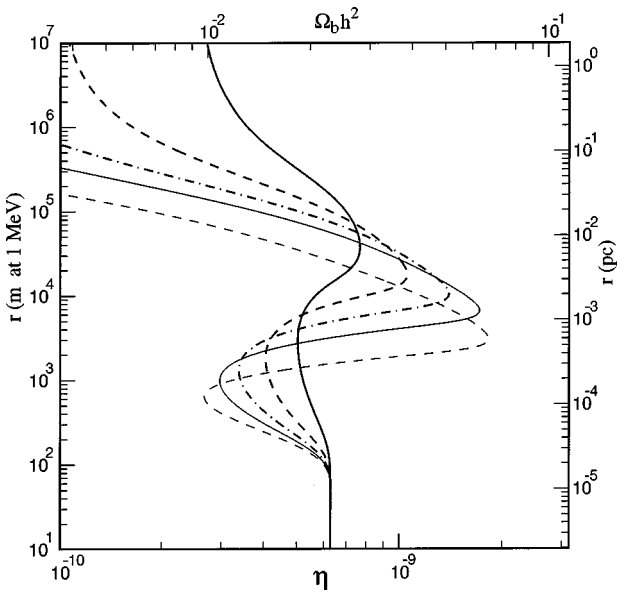

FIG. 4. Conservative upper limit to η from $Y_p \leqslant 0.248$ and $\mathrm{D/H} \geqslant 1.5 \times 10^{-5}$. The plot is for the c.c. geometry: the thick curves are for $f_r = 1/\sqrt{2}$ (solid line), 1/2 (dashed line), $1/2\sqrt{2}$ (dot-dashed line), and the thin curves are for $f_r = 1/4$ (solid line) and $f_r = 1/8$ (dashed line). The allowed region is to the left of each curve.

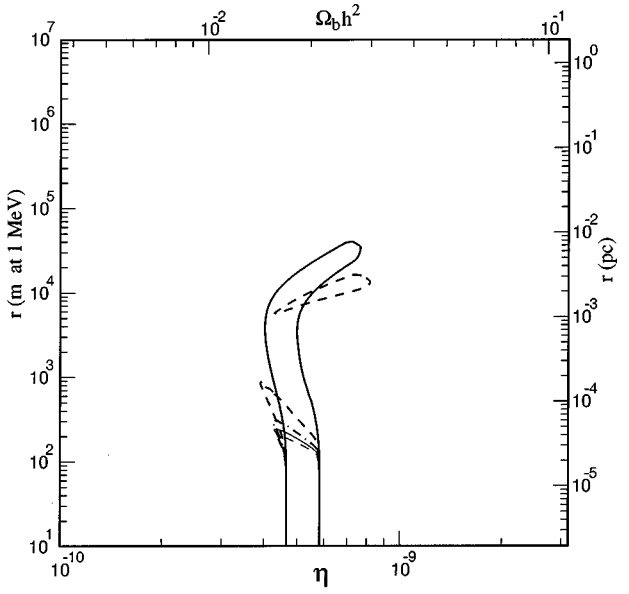

FIG. 5. The regions in the (r,η) plane allowed by D/H = $3.4 \pm 0.6 \times 10^{-5}$, $Y_p \leqslant 0.248$, and $\log_{10}{}^7\mathrm{Li/H} = -9.45 \pm 0.20$. The meaning of the different line styles is the same as in Fig. 4.

as our constraint. For ^{4}He we continue to use the Izotov-Thuan [15] upper limit $Y_p \leqslant 0.248$ and for ^{7}Li we use the range of Pinsonneault *et al.* [25]:

$$\log_{10}(^7\mathrm{Li/H})_p = -9.45 \pm 0.20. \tag{24}$$

The results for this set are displayed in Fig. 5.

In SBBN these constraints lead to a baryon density in the narrow range $\eta_{10} = 4.6 - 5.8$. In IBBN the allowed range is

$$\eta_{10} = 3.9 - 8.2 \quad (\eta_{10} = 3.7 - 10.5) \tag{25}$$

for the c.c. (s.s.) geometry.

In our third set we consider the case for low η in SBBN [12]. (See Fig. 6.) The 2σ OSS97 limits for Y_p,

$$0.224 \leqslant Y_p \leqslant 0.236, \tag{26}$$

correspond to ^{7}Li near the Spite plateau and a large primordial D. Hence we here use a conservative upper limit to D,

$$\mathrm{D/H} \leqslant 2.5 \times 10^{-4}, \tag{27}$$

and the Vauclair-Charbonnel [26] upper limit for ^{7}Li,

$$\log_{10}{}^7\mathrm{Li/H} \leqslant -9.55. \tag{28}$$

The results for this set are given in Fig. 6. The SBBN range is $\eta_{10} = 1.5 - 2.1$ (lower limit from D/H, upper limit from Y_p). The IBBN upper limits are higher:

$$\eta_{10} \leqslant 3.6 \quad (3.8). \tag{29}$$

We finally demonstrate that IBBN can alleviate the tension between low ^{4}He and low D. If we use the constraints

$$Y_p \leqslant 0.238 \quad (\mathrm{SBBN} \quad \eta_{10} \leqslant 2.4), \tag{30}$$

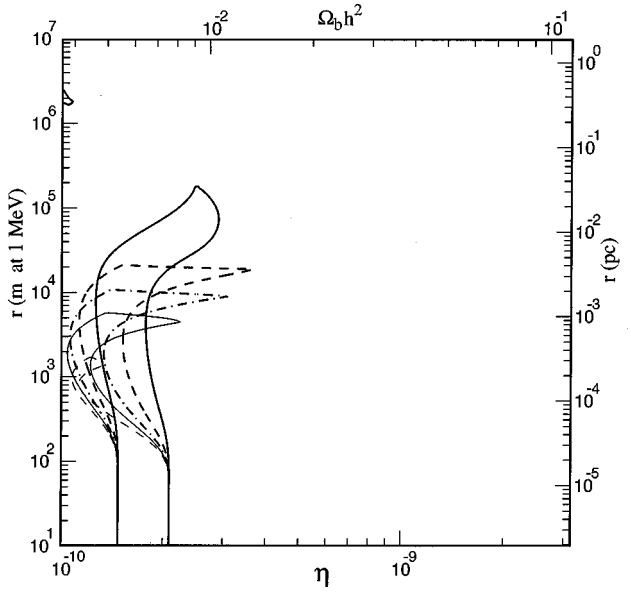

FIG. 6. The case for low η. This figure is similar to Fig. 5, but the constraints used are $Y_p = 0.230 \pm 0.006$, $\mathrm{D/H} \leqslant 2.5 \times 10^{-4}$, and $\log_{10}{}^7\mathrm{Li/H} \leqslant -9.55$.

$$\mathrm{D/H} \leqslant 10^{-4} \quad (\mathrm{SBBN} \quad \eta_{10} \geqslant 2.6), \tag{31}$$

$$\log_{10}{}^7\mathrm{Li/H} \leqslant -9.25 \quad (\mathrm{SBBN} \quad \eta_{10} \leqslant 8.3), \tag{32}$$

no value of η is allowed in SBBN (the ''crisis''). However, as shown in Fig. 7, some IBBN models satisfy these con-

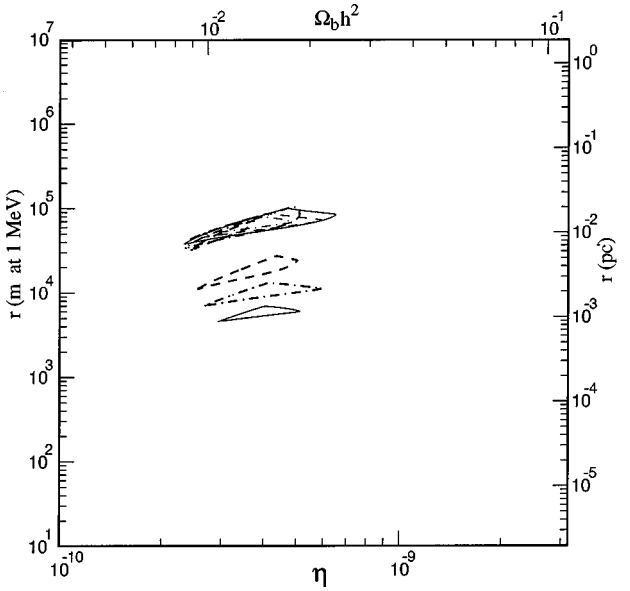

FIG. 7. Alleviating the BBN ''crisis.'' This figure is similar to Figs. 5 and 6, but the constraints used are $Y_p \leqslant 0.238$, $\mathrm{D/H} \leqslant 10^{-4}$, and $^7\mathrm{Li/H} \leqslant 10^{-9.25}$. These constraints are incompatible with each other in SBBN, but are compatible in IBBN with the optimal distance scale. The allowed regions for the two geometries are shown in the same plot. The ones for the s.s. geometry are all at the same distance scale. For the c.c. geometry we get allowed regions for three of the considered volume fractions, and they lie below the s.s. regions.

straints, with $2.6 \leqslant \eta_{10} \leqslant 6.0$ (c.c.) or $2.3 \leqslant \eta_{10} \leqslant 6.5$ (s.s.), in a narrow (about a factor of 2) range of the inhomogenity distance scale r. This is the ''optimum'' distance scale, which for these values of η varies between 5 km and 30 km (at 1 MeV) for the centrally condensed geometry. Similar solutions were found with r about 70 km for the spherical shell geometry, proving that the result essentially depends only on the scale and is robust against using different geometries.

V. CONCLUSIONS

We have studied the possibility of inhomogenous nucleosynthesis on the basis of the new observational situation, paying attention to the particular mechanisms capable of producing the inhomogeneities in the very early universe.

First we studied the typical foamlike inhomogeneity generated during the electroweak phase transition, which we modeled by using spherical symmetry with thin shells of high-density regions. We find that the scale from the EW transition tends to be too small to cause large deviations from SBBN predictions; that is, the bound on η is not significantly changed. However, the effects on theoretical yields *can be* of equal size or larger than some of the more detailed corrections recently included into the SBBN computations. As a result of the genericity of the EW inhomogeneities, these corrections may be viewed as setting the scale of accuracy achievable in SBBN computations.

Second, we considered the full parameter space of the IBBN models in both centrally condensed (QCD-type) and spherical shell (EW-type) geometries.

To answer the first question posed at the end of Sec. II: IBBN models can satisfy the observational constraints equally well and, for some small region of the parameter space, even better than SBBN. For inhomogeneities with distance scales near the ''optimum'' scale $r_{\rm opt}$, where the inhomogeneity effects are maximized, this agreement is obtained for a larger baryon density than in SBBN; precise values depend *intrinsically* on the observational constraints, but the upper limit to η from the upper limit to ^{4}He and from the lower limit to D/H may be raised by a factor of 2–3, whereas upper limits set by the ^{7}Li/H data are raised less, at most by a factor of 1.4. However, it is not possible ever to get η large enough to make $\Omega_b = 1$. For smaller scales the agreement is obtained for similar or slightly smaller values of η as in SBBN.

Regarding the second question, this optimum distance scale is not only larger than the EWPT horizon, but it is also several orders of magnitude larger than the QCD transition distance scale favored by QCD lattice calculations of the surface tension and the latent heat. However, the uncertainty in these values is as large as the values themselves so that a much smaller latent heat, leading to a larger distance scale, is still allowed; thus we cannot presently rule out the possibility of reaching the optimum inhomogeneity distance scale in the QCD transition.

There is a region of parameter space, where the tension between ^{4}He and D/H is alleviated compared to SBBN. This takes place if the inhomogeneity distance scale is close to $r_{\rm opt}$. The effect is however rather small, and for a low deuterium, say $\mathrm{D/H} \leqslant 5 \times 10^{-5}$, we cannot accommodate less helium than $Y_p = 0.240$; so IBBN cannot present itself as a solution to a dicothomy in observations. Since we also pointed out that the present Kamiokande result rules out the simplest particle physics solution to possible tension in SBBN, the conclusion that the problems are probably associated with the observations is bolstered.

ACKNOWLEDGMENT

We thank the Center for Scientific Computing (Finland) for computational resources.

[1] D. N. Schramm and R. V. Wagoner, Annu. Rev. Nucl. Sci. **27**, 37 (1977); A. M. Boesgaard and G. Steigman, Annu. Rev. Astron. Astrophys. **23**, 319 (1985); K. A. Olive and D. N. Schramm, in Particle Data Group, R. M. Barnett *et al.*, Phys. Rev. D **54**, 1 (1996), p. 109; B. E. J. Pagel, *Nucleosynthesis and Chemical Evolution of Galaxies* (Cambridge University Press, Cambridge, England, 1997); D. N. Schramm and M. S. Turner, Rev. Mod. Phys. **70**, 303 (1998).

[2] T. P. Walker, G. Steigman, D. N. Schramm, K. A. Olive, and H.-S. Kang, Astrophys. J. **376**, 51 (1991).

[3] M. S. Smith, L. H. Kawano, and R. A. Malaney, Astrophys. J. Suppl. Ser. **85**, 219 (1993).

[4] C. J. Copi, D. N. Schramm, and M. S. Turner, Phys. Rev. Lett. **75**, 3981 (1995).

[5] P. J. Kernan and L. M. Krauss, Phys. Rev. Lett. **72**, 3309 (1994).

[6] F. W. Stecker, Phys. Rev. Lett. **44**, 1237 (1980); K. A. Olive and M. S. Turner, *ibid.* **46**, 516 (1981); S. P. Riley and J. M. Irvine, J. Phys. G **17**, 35 (1991); G. M. Fuller, R. N. Boyd, and J. D. Kalen, Astrophys. J. Lett. **371**, L11 (1991); K. A. Olive, G. Steigman, and T. P. Walker, *ibid.* **380**, L1 (1991).

[7] D. A. Dicus, E. W. Kolb, A. M. Gleeson, E. C. G. Sudarshan, V. L. Teplitz, and M. S. Turner, Phys. Rev. D **26**, 2694 (1982).

[8] K. A. Olive, G. Steigman, and E. D. Skillman, Astrophys. J. **483**, 788 (1997).

[9] J. L. Linsky *et al.*, Astrophys. J. **402**, 694 (1993).

[10] G. Steigman and M. Tosi, Astrophys. J. **401**, 150 (1992); N. Hata, R. J. Scherrer, G. Steigman, D. Thomas, and T. P. Walker, *ibid.* **458**, 637 (1996); G. Steigman and M. Tosi, *ibid.* **453**, 173 (1995); M. Tosi, G. Steigman, F. Matteucci, and C. Chiappini, *ibid.* **498**, 226 (1998).

[11] N. Hata, R. J. Scherrer, G. Steigman, D. Thomas, T. P. Walker, S. Bludman, and P. Langacker, Phys. Rev. Lett. **75**, 3977 (1995).

[12] B. D. Fields, K. Kainulainen, K. A. Olive, and D. Thomas, New Astron. **1**, 77 (1996).

[13] S. T. Scully, M. Cassé, K. A. Olive, D. N. Schramm, J. Truran, and E. Vangioni-Flam, Astrophys. J. **462**, 960 (1996); S. Scully, M. Cassé, K. A. Olive, and E. Vangioni-Flam, *ibid.* **476**, 521 (1997); D. Galli, L. Stanghellini, M. Tosi, and F. Palla, *ibid.* **477**, 218 (1997).
[14] D. Sasselov and D. Goldwirth, Astrophys. J. Lett. **444**, L5 (1995); P. J. Kernan and S. Sarkar, Phys. Rev. D **54**, R3681 (1996); G. Steigman, S. M. Viegas, and R. Gruenwald, Astrophys. J. **490**, 187 (1997).
[15] Yu. I. Izotov and T. X. Thuan, Astrophys. J. **497**, 227 (1998); Astrophys. J. **500**, 188 (1998).
[16] E. Terlevich, presented at ''Synthesis of Light Nuclei in the Early Universe,'' ECT*, Trento, Italy, 1997.
[17] M. Kawasaki, P. Kernan, H.-S. Kang, R. J. Scherrer, G. Steigman, and T. P. Walker, Nucl. Phys. **B419**, 105 (1994); M. Kawasaki, K. Kohri, and K. Sato, Phys. Lett. B **430**, 132 (1998).
[18] Super-Kamiokande Collaboration, Y. Fukuda *et al.*, Phys. Lett. B **436**, 33 (1998).
[19] K. Enqvist, K. Kainulainen, and M. Thomson, Nucl. Phys. **B373**, 498 (1992); Phys. Lett. B **288**, 145 (1992).
[20] N. Terasawa and K. Sato, Phys. Lett. B **185**, 412 (1987); K. Enqvist, K. Kainulainen, and M. Thomson, Phys. Rev. Lett. **68**, 744 (1992).
[21] S. Dodelson, G. Gyuk, and M. S. Turner, Phys. Rev. D **49**, 5068 (1994).
[22] S. Hannestad, Phys. Rev. D **57**, 2213 (1998).
[23] F. Spite and M. Spite, Astron. Astrophys. **115**, 357 (1982); Nature (London) **297**, 483 (1992); M. Spite, P. François, P. E. Nissen, and F. Spite, Astron. Astrophys. **307**, 172 (1996).
[24] P. Bonifacio and P. Molaro, Mon. Not. R. Astron. Soc. **285**, 847 (1997).
[25] M. H. Pinsonneault, T. P. Walker, G. Steigman, and V. K. Narayanan, astro-ph/9803073.
[26] S. Vauclair and C. Charbonnel, Astrophys. J. **502**, 372 (1998).
[27] S. Burles and D. Tytler, astro-ph/9803071.
[28] A. Songaila, E. J. Wampler, and L. L. Cowie, Nature (London) **385**, 137 (1997); A. Songaila, astro-ph/9709293; S. Burles and D. Tytler, Astron. J. **114**, 1330 (1997); S. A. Levshakov, W. H. Kegel, and F. Takahara, Astrophys. J. Lett. **499**, L1 (1998).
[29] J. K. Webb, R. F. Carswell, K. M. Lanzetta, R. Ferlet, M. Lemoine, A. Vidal-Madjar, and D. V. Bowen, Nature (London) **388**, 250 (1997); astro-ph/9710089.
[30] J. H. Applegate, C. J. Hogan, and R. J. Scherrer, Phys. Rev. D **35**, 1151 (1987); H. Kurki-Suonio, R. A. Matzner, J. M. Centrella, T. Rothman, and J. R. Wilson, *ibid.* **38**, 1091 (1988); G. J. Mathews, B. S. Meyer, C. R. Alcock, and G. M. Fuller, Astrophys. J. **358**, 36 (1990); K. Jedamzik, G. M. Fuller, and G. J. Mathews, *ibid.* **423**, 50 (1994).
[31] H. Kurki-Suonio and R. A. Matzner, Phys. Rev. D **42**, 1047 (1990).
[32] H. Kurki-Suonio, R. A. Matzner, K. A. Olive, and D. N. Schramm, Astrophys. J. **353**, 406 (1990); B. S. Meyer, C. R. Alcock, G. J. Mathews, and G. M. Fuller, Phys. Rev. D **43**, 1079 (1991); G. J. Mathews, T. Kajino, and M. Orito, Astrophys. J. **456**, 98 (1996); M. Orito, T. Kajino, R. N. Boyd, and G. J. Mathews, *ibid.* **488**, 515 (1997).
[33] D. Thomas, D. N. Schramm, K. A. Olive, G. J. Mathews, B. S. Meyer, and B. D. Fields, Astrophys. J. **430**, 291 (1994).
[34] E. Witten, Phys. Rev. D **30**, 272 (1984).
[35] J. H. Applegate and C. J. Hogan, Phys. Rev. D **31**, 3037 (1985); H. Kurki-Suonio, *ibid.* **37**, 2104 (1988); M. B. Christiansen and J. Madsen, *ibid.* **53**, 5446 (1996).
[36] J. Ignatius, K. Kajantie, H. Kurki-Suonio, and M. Laine, Phys. Rev. D **50**, 3738 (1994).
[37] V. A. Rubakov and M. E. Shaposhnikov, Phys. Usp. **39**, 461 (1996).
[38] D. Comelli, M. Pietroni, and A. Riotto, Phys. Rev. D **50**, 7703 (1994).
[39] M. Giovannini and M. E. Shaposhnikov, Phys. Rev. Lett. **80**, 22 (1998); Phys. Rev. D **57**, 2186 (1998).
[40] J. B. Rehm and K. Jedamzik, Phys. Rev. Lett. **81**, 3307 (1998).
[41] H. Kurki-Suonio and E. Sihvola (in progress).
[42] A. E. Nelson, D. B. Kaplan, and A. G. Cohen, Nucl. Phys. **B373**, 453 (1991); G. R. Farrar and M. E. Shaposhnikov, Phys. Rev. D **50**, 774 (1994); J. M. Cline, K. Kainulainen, and A. Visher, *ibid.* **54**, 2451 (1996).
[43] A. F. Heckler, Phys. Rev. D **51**, 405 (1995).
[44] M. Joyce, T. Prokopec, and N. Turok, Phys. Rev. D **53**, 2958 (1996); J. M. Cline, M. Joyce, and K. Kainulainen, Phys. Lett. B **417**, 79 (1998).
[45] J. Cline, M. Joyce, and K. Kainulainen (in progress).
[46] G. D. Moore and T. Prokopec, Phys. Rev. D **52**, 7182 (1995).
[47] H. Kurki-Suonio and M. Laine, Phys. Rev. Lett. **77**, 3951 (1996).
[48] G. M. Fuller, K. Jedamzik, G. J. Mathews, and A. Olinto, Phys. Lett. B **333**, 135 (1994).
[49] M. Laine and K. Rummukainen, Phys. Rev. Lett. **80**, 5259 (1998); Nucl. Phys. **B535**, 423 (1998).
[50] QCDPAX Collaboration, Y. Iwasaki *et al.*, Phys. Rev. D **46**, 4657 (1992); B. Grossmann and M. L. Laursen, Nucl. Phys. **B408**, 637 (1993); Y. Iwasaki, K. Kanaya, L. Kärkkäinen, K. Rummukainen, and T. Yoshié, Phys. Rev. D **49**, 3540 (1994).
[51] R. Lopez, M. Turner, and G. Gyuk, Phys. Rev. D (to be published), astro-ph/9807279.